には Perkin Elmer 社「Operetta」を利用し、実験者のバイアスが入らないよう留意した。

C．研究結果

● 肥大型心筋症患者の iPS 由来心筋細胞
スクリーニングに利用するための指標を同定することを目的として、肥大型心筋症患者の中でも表現型が強く出現することが期待される乳児期発症例から樹立した iPS 細胞を心筋細胞へと分化誘導し、Operetta を用いて健常ボランティアから樹立した iPS 細胞を分化誘導した心筋細胞と比較した。肥大型心筋症患者 iPS 細胞から分化誘導した心筋細胞は、肥大型心筋症患者の心臓と同様、心筋細胞肥大が認められており、iPS 細胞を用いることで疾患表現型を再現できると考えられた。

● 心室型心筋細胞の選別
心房型ミオシン軽鎖で染色される心房筋と心室型ミオシン軽鎖で染色される心室筋では肥大の程度などの解析パラメータが大きく異なっていた。

● 培養基質および細胞数
CellCarrier をゼラチン（Sigma 社）、コラーゲン（Sigma 社）、肉腫由来成分（Geltrex：Thermo Scientific 社）でコーティングした上で iPS 由来心筋細胞を様々な細胞密度（１００個から６，０００個／ｃｍ^2）で播種した。コラーゲンおよび肉腫由来成分でコーティングした場合に plating efficiency が良好であったが、心筋細胞が線維芽細胞のように広く伸展された形態をとることから、疾患特異的な表現型が失われてしまう可能性が考えられた。ゼラチンでコーティングした場合および Perkin Elmer 社が細胞培養用に開発した加工表面上に細胞を播種した場合、接着細胞数は少ないものの個々の心筋細胞の形態が保たれていた。細胞密度が低過ぎる場合には、心筋細胞が線維芽細胞様に伸展された形態をとる一方、細胞密度が濃過ぎる場合には細胞同士が密に接着してしまい、いずれの場合においても細胞の形態を解析するためには不適であることが明らかになった。

● 複数 iPS 細胞を利用したバリデーション
健常ボランティア１名、健常血縁者１名、肥大型心筋症患者５名から樹立した iPS 細胞をそれぞれ２クローンずつ選択し、計 14 クローンを、全く同一のプロトコル・スケジュールで 3 回以上心筋細胞への分化誘導およびハイコンテンツ解析を行ったところ、肥大型心筋症 iPS 由来心筋細胞に共通して有意な変化が認められるパラメータを二つ得ることができた。

● 市販ライブラリーのスクリーニング
構築したスクリーニング系を用いて市販ライブラリー（８０化合物）のスクリーニングを実施した。肥大型心筋症患者４名から樹立した iPS 細胞から分化誘導した心筋細胞を用いてスクリーニングを実施したところ、発症年齢が乳児期の症例と成人の症例では、細胞レベルの異常を修正する効果が認められる化合物のパターンが異なっていた。

D．考察

● 心室型心筋細胞の選別
心筋症において症状が出現するのは心室であることから、ハイコンテンツ解析を行う際には心室型ミオシン軽鎖で免疫染色を行って心室筋を選別して解析することでより正確で S/N 比の大きな評価が可能になると考えられた。

● 培養基質および細胞数
培養基質および播種する心筋細胞の播種密度を最適化することで、安定して肥大型心筋症 iPS 由来心筋細胞の疾患特異的表現型を確認することができるスクリーニング系を構築できた。

● 複数 iPS 細胞を利用したバリデーション
複数 iPS 細胞を利用したバリデーションの結果、肥大型心筋症 iPS 由来心筋細胞に共通して有意な変化が認められるパラメータを得ることができ、**疾患表現型が強くする出現するクローンを選定することで、S/N 比の高い、高品質なスクリーニング系を構築できると考えられた。**

● 市販ライブラリーのスクリーニング

発症年齢が乳児期の症例と成人の症例では、細胞レベルの異常を修正する効果が認められる化合物のパターンが異なっていた。発症年齢が乳児期の特殊な症例では疾患表現型が比較的明瞭に出現するものの、より一般的な症例から樹立した iPS 細胞をスクリーニングに利用することでより多くの患者に対して治療効果を期待できる化合物を同定できる可能性が示された。

E．結論

疾患発症メカニズムへのエピジェノミックな要素が小さく、疾患表現型が明瞭であることが期待される乳児期発症例から樹立した iPS 細胞を用いてスクリーニング系を構築し、より一般的な症例から樹立した iPS 細胞を用いてバリデーションを行うことで、S/N 比の高いスクリーニング系を構築することができた。今後は疾患表現型が強くする出現するクローンを選定することで、さらに高品質なスクリーニング系を構築し、製薬企業と共同で革新的な治療薬開発を目指す。

F．研究発表

論文

1. Liu ML, Nagai T, Tokunaga M, Iwanaga K, Matsuura K, Takahashi T, Kanda M, Kondo N, Naito AT, Komuro I, Kobayashi Y. (2014). Anti-inflammatory peptides from cardiac progenitors ameliorate dysfunction after myocardial infarction. J Am Heart Assoc. 3(6):e001101.
2. Yasui H, Lee JK, Yoshida A, Yokoyama T, Nakanishi H, Miwa K, Naito AT, Oka T, Akazawa H, Nakai J, Miyagawa S, Sawa Y, Sakata Y, Komuro I. (2014). Excitation propagation in three-dimensional engineered hearts using decellularized extracellular matrix. Biomaterials. 35(27):7839-50.
3. Kudo-Sakamoto Y, Akazawa H, Ito K, Takano J, Yano M, Yabumoto C, Naito AT, Oka T, Lee JK, Sakata Y, Suzuki J, Saido TC, Komuro I. (2014). Calpain-dependent cleavage of N-cadherin is involved in the progression of post-myocardial infarction remodeling. J Biol Chem. 2014 289(28):19408-19.
4. Sumida T, Naito AT, Nomura S, Nakagawa A, Higo T, Hashimoto A, Okada K, Sakai T, Ito M, Yamaguchi T, Oka T, Akazawa H, Lee JK, Minamino T, Offermanns S, Noda T, Botto M, Kobayashi Y, Morita H, Manabe I, Nagai T, Shiojima I, Komuro I. (2015) Complement C1q-induced activation of β-catenin signalling causes hypertensive arterial remodelling. Nat Commun. 6:6241. doi: 10.1038/ncomms7241.

学会発表

国内学会

1. 内藤篤彦：iPS 細胞を用いた循環器疾患に対する創薬、For the Better Forum 2014 (2014, 9, 東京)
2. 内藤篤彦：Drug Discovery Against Heart Failure using Human iPS cells. 、第 18 回日本心不全学会学術集会（2014, 10, 大阪）
3. 岡田佳築、内藤篤彦、塩島一朗、坂田泰史、小室一成：Wnt/β-catenin Signaling Promotes Heart Failure-Induced Skeletal Myopathy through Direct Interaction with FoxO.、第 18 回日本心不全学会学術集会（2014, 10, 大阪）
4. 内藤篤彦：Wnt シグナルと心臓の生老病死、第６６回日本皮膚科学会西部支部学術集会（2014, 11, 高松）
5. 内藤篤彦：Wnt シグナルと心臓の生老病死、脳心血管抗加齢研究会 2014（2014, 12, 大阪）

国際学会

1. Akito Nakagawa, Atsuhiko Naito, Tomokazu Sumida, Seitaro Nomura, Masato Shibamoto, Tomoaki Higo, Katsuki Okada, and Issei Komuro: Activation of canonical Wnt signaling in arterial endothelial cell induces cardiac dysfunction. The 18th International Vascular Biology Meeting (2014, 4, Kyoto)
2. Tomoaki Higo, Atsuhiko Naito, Yasushi Sakata, and Issei Komuro: Pathogenic role of DNA single strand break accumulation in heart failure. Basic Cardiovascular Sciences Scientific Sessions (2014, 7, Las Vegas)
3. Yuki Kuramoto, Masamichi Ito, and Atsuhiko Naito: Non-genetic method for purification of ventricular cells from human iPS-derived cardiomyocytes. Safety Pharmacology Society Annual Meeting (2014, 10, Washington DC)
4. Masamichi Ito, Yuki Kuramoto, and Atsuhiko Naito: Scalable, reproducible, and echonomical method for producing cardiomyocytes from human iPS cells. Safety Pharmacology Society Annual

Meeting (2014, 10, Washington DC)

5. Masamichi Ito, Ryoko Takizawa, Natsumi Igarashi, Megumi Naito, Issei Komuro, and Atsuhiko Naito: Scalable, reproducible, and echonomical method for producing cardiomyocytes from human iPS cells. American Heart Association Scientific Sessions 2014 (2014, 11, Chicago)

G．知的所有権の取得状況

特許

1.

出願日：2014年10月9日

出願番号：特願2014-208147

発明の名称：心筋細胞の製造方法、心室型心筋細胞及びその製造方法、並びにスクリーニング方法

発明者：内藤篤彦、小室一成

様式第１９

学　会　等　発　表　実　績

委託業務題目「ゲノム解析技術および疾患特異的iPS細胞を用いた心筋症に対する革新的な医薬品開発研究」
機関名　国立大学法人　東京大学

１．学会等における口頭・ポスター発表

発表した成果（発表題目、口頭・ポスター発表の別）	発表者氏名	発表した場所（学会等名）	発表した時期	国内・外の別
Angiogenic therapy for heart failure(口頭)	小室　一成	China-Japan Conference	2014/4/15	国内
Activation of canonical Wnt signaling in arterial endothelial cell induces cardiac dysfunction(ポスター)	Akito Nakagawa, Atsuhiko Naito, Tomokazu Sumida, Seitaro Nomura, Masato Shibamoto, Tomoaki Higo, Katsuki Okada, and Issei Komuro	The 18th International Vascular Biology Meeting	2014/4/15	国内
心不全の新しい治療(口頭)	小室　一成	日本麻酔科学会	2014/5/16	国内
P13 Kinase signaling and heart failure(口頭)	小室　一成	Heart Failure 2014	2014/5/19	国外
Stem cells & cardiac regeneration(口頭)	Issei Komuro	The 8th OCC 2014	2014/5/30	国外
Cooperative epigenomic switch during cardiomyocyte differentiation	Hiroyuki Aburatani	国立遺伝学研究所研究会	2014/6/27	国内
Pathogenic role of DNA single strand break accumulation in heart failure.(ポスター)	Tomoaki Higo, Atsuhiko Naito, Yasushi Sakata, and Issei Komuro.	Basic Cardiovascular Sciences Scientific Sessions	2014/7/16	国外
Molecular Mechanisms of Heart Failure(口頭)	Issei Komuro	The 12th China Congress of ISHR	2014/8/15	国外
Cooperative epigenomic switch during cardiomyocyte differentiation	Hiroyuki Aburatani	Cold Spring Harbor Asia Conference on Systems Biology of gene	2014/9/9	国外
Myocardial Natriuretic Peptide Signaling In Heart Failure: Basic Insights(口頭)	Issei Komuro	2014 HFSA Annual Scientific Meeting	2014/9/16	国外
Wnt/β-catenin Signaling Promotes Heart Failure-Induced Skeletal Myopathy through Direct Interaction with FoxO(ポスター)	岡田佳築、内藤篤彦、塩島一朗、坂田泰史、小室一成	第18回日本心不全学会学術集会	2014/10/12	国内

Molecular Mechanisms of Heart Failure(口頭)	Issei Komuro	3rd International Conference on Cardiovascular Science	2014/10/14	国外
Scalable, reproducible, and echonomical method for producing cardiomyocytes from human iPS cells(ポスター)	Masamichi Ito, Ryoko Takizawa, Natsumi Igarashi, Megumi Naito, Issei Komuro, and Atsuhiko Naito	American Heart Association Scientific Sessions 2014	2014/11/18	国外
Molecular analysis of RASopathies using next generation sequencer	Aoki Y, Niihori T, Inoue SI and Matsubara Y	The 14 th East Asian Union of Human Genetics (EAUHGS) Annual Meeting	2014/11/20	国内
心不全の病態解明を目指した不全心筋サンプルを用いた観察研究	Asakura M, Asanuma H, Ito S, Min KD, Seguchi O, Nishigori M, Nakatani T, Tomonaga T, Minamino N, Kitakaze M	第18回日本心不全学会学術集会	2014/10/10	国内
圧負荷心不全モデルマウスにおける腎臓の遺伝子変化	Sindow K, Asakura M, Min KD, Imazu M, Fukuda H, Kitakaze M	第18回日本心不全学会学術集会	2014/10/10	国内
Mtus1 splice variant inhitits cardiac hypertrophy and exacerbates heart failure.	Ito S, Asakura M, Min KD, Imazu M, Shindo K, Asanuma H, Kitakaze M	ESC Congress 2014	2014/8/30	国外
Pressure overload to the heart induces pulmonary up-regulation of genes coding secretory proteins involved in the cardiovascular diseases.	Min KD, Asakura M, Ito S, Imazu M, Shindo K, Asanuma H, Kitakaze M	ESC Congress 2014	2014/8/30	国外
Temporal and quantitative regulation of Smad9 by its wpecific ligase Asb2 is required for cardiac development through the induction of Tbx2 expression by BMP2 stimulation.	Min KD, Asakura M, Ito S, Imazu M, Shindo K, Kitakaze M	AHA 2014	2014/11/15	国外
Effects of the oral adsorbent of AST-120 in patients with both chronic heart failue and chronic kidney disease.	Imazu M, Asakura M, Hasegawa T, Asanuma H, Ito S, Nakano A, Funada A, Sugano Y, Ohara T, Kanzaki H, Takahama H, Morita T, Anzai T, Kitakaze M	AHA 2014	2014/11/15	国外

Coordinated chromatin regulation by developmental signals during cardiomyocyte differentiation	Hiroyuki Aburatani	Joing symposium on TGF-b family and cancer	2015/1/13	国内

２．学会誌・雑誌等における論文掲載

掲載した論文（発表題目）	発表者氏名	発表した場所（学会誌・雑誌等名）	発表した時期	国内・外の別
Noninvasive and quantitative live imaging reveals a potential stress-responsive enhancer in the failing heart	Matsuoka K, Asano Y, Higo S, Tsukamoto O, Yan Y, Yamazaki S, Matsuzaki T, Kioka H, Kato H, Uno Y, Asakura M, Asanuma H, Minamino T, Aburatani H, Kitakaze M, Komuro I, Takashima S.I	FASEB J	2014年4月	国外
Dickkopf-3: a stubborn protector of cardiac hypertrophy.	Akazawa H, Komuro I.	Cardiovasc Res	2014年4月	国外
Src is required for mechanical stretch-induced cardiomyocyte hypertrophy through angiotensin II type	Wang S, Gong H, Jiang G, Ye Y, Wu J, You J, Zhang G, Sun A, Komuro	PLoS One	2014年4月	国外
Recurrent gain-of-function mutations of RHOA in diffuse-type gastric carcinoma.	Kakiuchi M, Nishizawa T, Ueda H, Gotoh K, Tanaka A, Hayashi A, Yamamoto S, Tatsuno K, Katoh H, Watanabe Y, Ichimura T, Ushiku T, Funahashi S, Tateishi K, Wada I, Shimizu N, Nomura S, Koike K, Seto Y, Fukayama M, Aburatani H, Ishikawa S.	Nat Genet.	2014年6月	国外

Knockdown of nucleosome assembly protein 1-like 1 induces mesoderm formation and cardiomyogenesis via Notch signaling in murine induced pluripotent stem cells.	Gong H, Yan Y, Fang B, Xue Y, Yin P, Li L, Zhang G, Sun X, Chen Z, Ma H, Yang C, Ding Y, Yong Y, Zhu Y, Yang H, Komuro I, Ge J, Zou Y	Stem Cells	2014年7月	国外
Comparison of 5-year survival after acute myocardial infarction using angiotensin-converting enzyme inhibitor versus angiotensin II receptor blocker.	Hara M, Sakata Y, Nakatani D, Suna S, Usami M, Matsumoto S, Sugitani T, Nishino M, Sato H, Kitamura T, Nanto S, Hamasaki T, Hori M, Komuro I; OACIS Investigators.	Am J Cardiol	2014年7月	国外
Myocardium-derived angiopoietin-1 is essential for coronary vein formation in the developing heart.	Arita Y, Nakaoka Y, Matsunaga T, Kidoya H, Yamamizu K, Arima Y, Kataoka-Hashimoto T, Ikeoka K, Yasui T, Masaki T, Yamamoto K, Higuchi K, Park JS, Shirai M, Nishiyama K, Yamagishi H, Otsu K, Kurihara H, Minami T, Yamauchi-Takihara K, Koh GY, Mochizuki N, Takakura N, Sakata Y, Yamashita JK, Komuro I.	Nature Communications	2014年7月	国外
Calpain-dependent Cleavage of N-cadherin Is Involved in the Progression of Post-myocardial Infarction Remodeling.	Kudo-Sakamoto Y, Akazawa H, Ito K, Takano J, Yano M, Yabumoto C, Naito AT, Oka T, Lee JK, Sakata Y, Suzuki JI, Saido TC, Komuro I	J Biol Chem	2014年7月	国外
Reduced risk of recurrent myocardial infarction in homozygous carriers of the chromosome 9p21 rs1333049 C risk allele in the contemporary percutaneous coronary intervention era: a prospective observational	Hara M, Sakata Y, Nakatani D, Suna S, Usami M, Matsumoto S, Ozaki K, Nishino M, Sato H, Kitamura T, Nanto S, Hamasaki T	BMJ Open	2014年8月	国外
The metabolic syndrome and DYRK1B.	Morita H, Komuro I.	N Engl J Med	2014年8月	国外

Excitation propagation in three-dimensional engineered hearts using decellularized extracellular matrix.	Yasui H, Lee JK, Yoshida A, Yokoyama T, Nakanishi H, Miwa K, Naito AT, Oka T, Akazawa H, Nakai J, Miyagawa S, Sawa Y, Sakata Y, Komuro I.	Biomaterials	2014年9月	国外
Mitochondrial Aldehyde Dehydrogenase 2 Plays Protective Roles in Heart Failure After Myocardial Infarction via Suppression of the Cytosolic JNK/p53 Pathway in Mice.	Sun A, Zou Y, Wang P, Xu D, Gong H, Wang S, Qin Y, Zhang P, Chen Y, Harada M, Isse T, Kawamoto T, Fan H, Yang P, Akazawa H, Nagai T, Takano H, Ping P, Komuro I, Ge J.	J Am Heart Assoc	2014年9月	国外
Effects of methylglyoxal on human cardiac fibroblast: Roles of transient receptor potential ankyrin 1 (TRPA1)channels.	Oguri G, Nakajima T, Yamamoto Y, Takano N, Tanaka T, Kikuchi H, Morita T, Nakamura F, Yamasoba T, Komuro I.	Am J Physiol Heart Circ Physiol	2014年11月	国外
Somatic mutations in cerebral cortical malformations.	Morita H,Komuro I.	N Engl J Med	2014年11月	国外
Anti-inflammatory peptides from cardiac progenitors ameliorate dysfunction after myocardial infarction.	Liu ML, Nagai T, Tokunaga M, Iwanaga K, Matsuura K, Takahashi T, Kanda M, Kondo N, Naito AT, Komuro I, Kobayashi Y.	J Am Heart Assoc.	2014年12月	国外

Trans-ancestry mutational landscape of hepatocellular carcinoma genomes.	Totoki Y, Tatsuno K, Covington KR, Ueda H, Creighton CJ, Kato M, Tsuji S, Donehower LA, Slagle BL, Nakamura H, Yamamoto S, Shinbrot E, Hama N, Lehmkuhl M, Hosoda F, Arai Y, Walker K, Dahdouli M, Gotoh K, Nagae G, Gingras MC, Muzny DM, Ojima H, Shimada K, Midorikawa Y, Goss JA, Cotton R, Hayashi A, Shibahara J, Ishikawa S, Guiteau J, Tanaka M, Urushidate T, Ohashi S, Okada N, Doddapaneni H, Wang M, Zhu Y, Dinh H, Okusaka T, Kokudo N, Kosuge T, Takayama T, Fukayama M, Gibbs RA, Wheeler DA, Aburatani H, Shibata T.	Nat. Genet	2014年12月	国外
Higd1a is a positive regulator of cytochrome c oxidase.	Hayashi T, Asano Y, Shintani Y, Aoyama H, Kioka H, Tsukamoto O, Hikita M, Shinzawa-Itoh K, Takafuji K, Higo S, Kato H, Yamazaki S, Matsuoka K, Nakano A, Asanuma H, Asakura M, Minamino T, Goto Y, Ogura T, Kitakaze M, Komuro I, Sakata Y, Tsukihara T, Yoshikawa S, Takashima S.	Proc Natl Acad Sci U S A	2015年2月	国外

Complement C1q-induced activation of b-catenin signalling causes hypertensive arterial remodelling.	Sumida T, Naito AT, Nomura S, Nakagawa A, Higo T, Hashimoto A, Okada K, Sakai T, Ito M, Yamaguchi T, Oka T, Akazawa H, Lee JK, Minamino T, Offermanns S, Noda T, Botto M, Kobayashi Y, Morita H, Manabe I, Nagai T, Shiojima I, Komuro I.	Nature Communications	2015年2月	国外
Coronary atherosclerotic lesions in patients with a ruptured abdominal aortic aneurysm.	Nakayama A, Morita H, Hamamatsu A, Miyata T, Hoshina K, Nagayama M, Takanashi S, Sumiyoshi T, Komuro I.	Heart and Vessels	In press	国外
Activating mutations in RRAS underlie a phenotype within the RASopathy spectrum and contribute to leukaemogenesis.	Flex E, Jaiswal M, Pantaleoni F, Martinelli S, Strullu M, Fansa EK, Caye A, De Luca A, Lepri F, Dvorsky R, Pannone L, Paolacci S, Zhang SC, Fodale V, Bocchinfuso G, Rossi C, Burkitt-Wright EM, Farrotti A, Stellacci E, Cecchetti S, Ferese R, Bottero L, Castro S, Fenneteau O, Brethon B, Sanchez M, Roberts AE, Yntema HG, van der Burgt I, Cianci P, Bondeson ML, Digilio MC, Zampino G, Kerr B, Aoki Y, Loh ML, Palleschi A, Di Schiavi E, Carè A, Selicorni A, Dallapiccola B, Cirstea IC, Stella L, Zenker	Hum Mol Genet	2014年8月	国外

PDE5 inhibitor efficacy is estrogen dependent in female heart disease.	Sasaki H, Nagayama T, Blanton RM, Seo K, Zhang M, Zhu G, Lee DI, Bedja D, Hsu S, Tsukamoto O, Takashima S, Kitakaze M, Mendelsohn ME, Karas RH, Kass DA, Takimoto E.	J Clin Invest	2014年6月	国外
Olmesartan prevents cardiac rupture in mice with myocardial infarction by modulating growth differentiation factor 15 and p53.	Chen BH, Lu D, Fu YJ, Zhang JW, Huang XB, Cao SP, Xu DL, Bin JP, Kitakaze M, Huang QB, Liao YL.	British Journal of Pharmacology	2014年8月	国外
Disruption of histamine H-2 receptor slows heart failure progression through reducing myocardial apoptosis and fibrosis.	Zeng Z, Shen L, Li XX, Luo T, Wei X, Zhang JW, Cao SP, Huang XB, Fukushima Y, Bin JP, Kitakaze M, Xu DL, Liao YL.	Clinical Science	2014年10月	国外
Pathophysiological impact of serum fibroblast growth factor 23 in patients with nonischemic cardiac disease and early chronic kidney disease.	Imazu M, Takahama H, Asanuma H, Funada A, Sugano Y, Ohara T, Hasegawa T, Asakura M, Kanzaki H, Anzai T, Kitakaze M.	AJP-Heart Circ Physiol	2014年11月	国外
Augmented AMPK activity inhibits cell migration by phosphorylating the novel substrate Pdlim5.	Yan Y, Tsukamoto O, Nakano A, Kato H, Kioka H, Ito N, Higo S, Yamazaki S, Shintani Y, Matsuoka K, Liao Y, Asanuma H, Asakura M, Takafuji K, Minamino T, Asano Y, Kitakaze M, Takashima S.	Nature communications	2015年1月	国外

（注１）発表者氏名は、連名による発表の場合には、筆頭者を先頭にして全員を記載すること。
（注２）本様式はexcel形式にて作成し、甲が求める場合は別途電子データを納入すること。

The FASEB Journal • Research Communication

Noninvasive and quantitative live imaging reveals a potential stress-responsive enhancer in the failing heart

Ken Matsuoka,[*,†] Yoshihiro Asano,[*,†,1] Shuichiro Higo,[*,†] Osamu Tsukamoto,[†] Yi Yan,[†] Satoru Yamazaki,[§] Takashi Matsuzaki,[*] Hidetaka Kioka,[*,†] Hisakazu Kato,[†] Yoshihiro Uno,[‡] Masanori Asakura,[‖] Hiroshi Asanuma,[¶] Tetsuo Minamino,[*] Hiroyuki Aburatani,[#] Masafumi Kitakaze,[‖] Issei Komuro,[*] and Seiji Takashima[*,†]

[*]Department of Cardiovascular Medicine and [†]Department of Medical Biochemistry and [‡]Laboratory of Reproductive Engineering, Institute of Experimental Animal Sciences, Osaka University Graduate School of Medicine, Suita, Japan; [§]Department of Cell Biology and [‖]Department of Clinical Research and Development, National Cerebral and Cardiovascular Center Research Institute, Suita, Japan; [¶]Department of Cardiovascular Science and Technology, Kyoto Prefectural University School of Medicine, Kyoto, Japan; and [#]Genome Science Division, Research Center for Advanced Science and Technology, University of Tokyo, Tokyo, Japan

ABSTRACT **Recent advances in genome analysis have enabled the identification of numerous distal enhancers that regulate gene expression in various conditions. However, the enhancers involved in pathological conditions are largely unknown because of the lack of *in vivo* quantitative assessment of enhancer activity in live animals. Here, we established a noninvasive and quantitative live imaging system for monitoring transcriptional activity and identified a novel stress-responsive enhancer of *Nppa* and *Nppb*, the most common markers of heart failure. The enhancer is a 650-bp fragment within 50 kb of the *Nppa* and *Nppb* loci. A chromosome conformation capture (3C) assay revealed that this distal enhancer directly interacts with the 5′-flanking regions of *Nppa* and *Nppb*. To monitor the enhancer activity in a live heart, we established an imaging system using the firefly luciferase reporter. Using this imaging system, we observed that the novel enhancer activated the reporter gene in pressure overload-induced failing hearts (failing hearts: 5.7±1.3-fold; sham-surgery hearts: 1.0±0.2-fold; $P<0.001$, repeated-measures ANOVA). This method will be particularly useful for identifying enhancers that function only during pathological conditions.—Matsuoka, K., Asano, Y., Higo, S., Tsukamoto, O., Yan, Y., Yamazaki, S., Matsuzaki, T., Kioka, H., Kato, H., Uno, Y., Asakura, M., Asanuma, H., Minamino, T., Aburatani, H., Kitakaze, M., Komuro, I., and Takashima, S. Noninvasive and quantitative live imaging reveals a potential stress-responsive enhancer in the failing heart. *FASEB J.* 28, 1870–1879 (2014). www.fasebj.org**

Key Words: natriuretic peptide · transcriptional regulation · in vivo *assessment*

GENE EXPRESSION IS REGULATED through the integrated action of many *cis*-regulatory elements, including core promoters, proximal promoters, distant enhancers, and insulators (1). Several methods have been used to explore the function of *cis*-regulatory elements during a variety of developmental stages (2, 3). However, the identification of gene regulatory elements with pathophysiological roles has been technically difficult because there are few appropriate models for monitoring transcriptional activity in live animals under pathological conditions.

Here, we focused on the regulatory elements that are responsive to heart failure. The natriuretic peptides, atrial natriuretic peptide (ANP) and brain natriuretic peptide (BNP), encoded by the neighboring genes *Nppa* and *Nppb* are activated in the embryonic heart, down-regulated after birth, and then reactivated during heart failure. Both peptides are well-known biomarkers that are strongly induced during heart failure and represent its severity. Cardiologists frequently use these peptides as natriuretic and vasorelaxant agents to treat various clinical conditions (4–8). Many studies have tried to elucidate the mechanisms of their transcriptional regulation because factors that regulate these

Abbreviations: 3C, chromosome conformation capture; ANP, atrial natriuretic peptide; BNP, brain natriuretic peptide; ChIP-seq, chromatin immunoprecipitation sequencing; CMV, cytomegalovirus; CR, conserved region; CTCF, CCCTC-binding factor; H3K4me1, histone H3 monomethylated at lysine 4; H3K4me3, histone H3 trimethylated at lysine 4; PE, phenylephrine; TAC, transverse aortic constriction

[1] Correspondence: Osaka University Graduate School of Medicine, 2-2 Yamadaoka, Suita, Osaka 565–0871, Japan. E-mail: asano@cardiology.med.osaka-u.ac.jp

doi: 10.1096/fj.13-245522

This article includes supplemental data. Please visit *http://www.fasebj.org* to obtain this information.

natriuretic peptides are potential therapeutic targets for heart disease (9–14).

Mice transgenic for various loci, including the 5′-flanking regions of the natriuretic peptide genes, have been used to identify the regulatory elements required for transcriptional activation either during heart development or in the diseased heart. These studies reported that the 5′-flanking regions of the natriuretic peptide genes regulated their expression during heart development (9, 10, 13); however, the 5′-flanking regions were not responsible for their specific reactivation in the diseased heart (11, 12). A recent study identified the distal enhancer elements regulating the natriuretic peptide genes in the developing heart by examining cardiac-specific transcription factor binding sites; however, these enhancer elements did not respond to heart failure (14). Therefore, the stress-responsive regulatory elements that function during heart failure have not yet been identified and are potentially located outside the 5′-flanking regions.

In this study, we aimed to identify the novel stress-responsive enhancer elements of the *Nppa* and *Nppb* genes in the failing heart. Furthermore, we established a noninvasive and quantitative live imaging assay to monitor the transcriptional activity of candidate enhancers in the failing heart. *In vivo* live imaging of the firefly luciferase reporter in a single mouse enabled us to analyze the sequential changes in enhancer activity during the progression of heart failure. Combined with a fine mapping technique using epigenetic markers, we identified a 650-bp stress-responsive enhancer that was strongly activated by cardiac hypertrophy and heart failure.

MATERIALS AND METHODS

Animals

All procedures were performed according to the U.S. National Institutes of Health (NIH) Guide for the Care and Use of Laboratory Animals (NIH publication no. 85-23, revised 1996) and were approved by the Animal Experiments Committee, Osaka University (approval no. 21-78-10).

Reagents and antibodies

Phenylephrine (PE) was purchased from Sigma-Aldrich (St. Louis, MO, USA). The anti-RNA polymerase II and anti-histone H3 trimethylated at lysine 4 (H3K4me3) antibodies used for chromatin immunoprecipitation sequencing (ChIP-seq) were kind gifts from Dr. H. Kimura (Graduate School of Frontier Biosciences, Osaka University).

Primary culture of neonatal rat cardiomyocytes

Ventricular myocytes obtained from 1- or 2-d-old Wistar rats were prepared and cultured overnight in Dulbecco's modified Eagle's medium (Sigma-Aldrich) containing 10% FBS, as described previously (15).

Comparative genomics

Genome-wide multiple alignments of the genomic sequences containing the *Nppa* and *Nppb* genes were performed using the University of California Santa Cruz (UCSC) Genome Browser (16); 8 vertebrate species were compared, including mouse (mm9, July 2007), rat (m4, Nov. 2004), human (hg18, Mar. 2006), orangutan (ponAbe2, July 2007), dog (canFam2, May 2005), horse (equCab1, Jan. 2007), opossum (monDom4, Jan. 2006), and chicken (galGal3, May 2006). We used vertebrate Multiz alignment of DNA sequences (17) to analyze the homology of DNA sequences among mouse and other species. We used the Placental Mammal Basewise Conservation assessed by PhyloP (18) to assess the degree of mammalian conservation. Next, we identified discrete conserved fragments. The transcribed sequences within the conserved set were filtered out using known genes, spliced ESTs, and mRNA annotations obtained from the UCSC genome browser. Finally, we manually curated the data set to remove any additional false positives by visual examination of the UCSC genomic data. We defined the noncoding conserved regions (CRs) that were homologous at least in the human and mouse genomes and at least 1 kb away from the transcription start sites as the enhancer candidates.

ChIP sequencing on mouse heart tissues

Whole hearts were isolated from 8-wk-old C57BL6 mice, perfused rapidly with cold PBS, flash-frozen in liquid nitrogen, homogenized using a sterile tissue grinder, and cross-linked with 0.3% paraformaldehyde. Subsequently, chromatin isolation, sonication, and immunoprecipitation using an anti-RNA polymerase II antibody and an anti-H3K4me3 antibody were performed. The ChIP DNA and input samples were sheared by sonication, end-repaired, ligated to the sequencing adapters, and amplified. The purified ChIP DNA library samples were sequenced using the Illumina Genome Analyzer II (Illumina, Inc., San Diego, CA, USA). Unfiltered sequence reads were aligned to the mouse reference genome [U.S. National Center for Biotechnology Information (NCBI) build 37, mm9] using Bowtie. RNA polymerase II- and H3K4me3-enriched regions were identified using MACS (19) with the default parameters.

Lentiviral enhancer assay

Eleven CRs were PCR amplified from the mouse BAC clone containing the *Nppa* and *Nppb* loci (clone RP23-128E8; BACPAC Resources Center, Children's Hospital Oakland, Oakland, CA, USA; primers and probes are listed in Supplemental Table S1). The PCR fragments were subcloned into the pCR-Blunt II-TOPO vector (Invitrogen, Carlsbad, CA, USA) and recombined into a lentiviral vector encoding the firefly luciferase reporter (pGreenFire Transcriptional Reporter Lentivector; System Biosciences, Mountain View, CA, USA). The lentiviral particles were produced by transfection of 293T cells with the 3 lentiviral packaging plasmids (*i.e.*, pMDLg/pRRE, pRSV-Rev, and pMD2.VSV.G) using Lipofectamine 2000 (Invitrogen). The supernatant from 293T cells containing the lentiviral particles was collected 48 h after transfection, sterilized using a 0.45-μm cellulose acetate filter, and concentrated by centrifugation (Peg-it Virus Precipitation Solution, System Biosciences).

Rat neonatal cardiomyocytes isolated as described above were plated in 96-well plates. The next day, the medium was replaced with a serum-free medium containing the lentiviral vector, and the cells were incubated for 12 h. Subsequently, the cardiomyocytes were exposed to 100 μM PE for 48 h prior to the luciferase assay.

RNA extraction and quantitative RT-PCR

The total RNA was prepared from rat cardiomyocytes, rat cardiac fibroblasts, murine hearts, and murine brains using the RNA-Bee RNA isolation reagent (Tel-Test, Friendswood, TX, USA) and then converted to cDNA using the high-capacity cDNA reverse transcription kit (Applied Biosystems, Foster City, CA, USA), according to the manufacturer's instructions. The quantitative RT-PCR was performed using the TaqMan technology and the StepOnePlus real-time PCR System (Applied Biosystems). All samples were processed in duplicate. The level of each transcript was quantified according to the threshold cycle (C_t) method using GAPDH as an internal control. Inventoried TaqMan gene expression assays were used: *Nppa*, Rn0056661, Mm01255748; *Nppb*, Rn00580641, Mm01255770; *Gapdh*, rodent GAPDH control reagent.

3C analysis

The whole hearts of the mice were isolated, perfused rapidly with cold PBS, flash-frozen in liquid nitrogen, homogenized using a sterile tissue grinder, and fixed with 1% paraformaldehyde. The cross-linked tissues utilized for 3C experiments were subjected to digestion with *Bam*HI following standard protocols (20, 21). The mouse BAC DNA containing *Nppa* and *Nppb* (clone RP23-128E8) was used as a control. The TaqMan real-time PCR was performed using probes near the restriction sites; the primers and probes are listed in Supplemental Table S2.

Transgenic mouse enhancer assay

The candidate enhancer regions were cloned into a vector encoding the minimal CMV promoter driving the luciferase gene as described above. Transgenic mouse embryos were generated by pronuclear injection into the zygotes of BDF1 mice using standard methods. Because black fur attenuates light transmission, albino mice were generated by crossing the transgenic founders to ICR albino mice.

In vivo bioluminescence imaging

Prior to *in vivo* imaging, the mice were anesthetized using isoflurane, and the black mice were shaved from the neck to the lower torso to allow the optimal visualization of fluorescence without interference from the black fur. A D-luciferin solution was injected intraperitoneally (150 mg/kg i.p.) or intravenously (75 mg/kg i.v.). The mice were imaged using an *in vivo* live imaging system (IVIS Lumina II; Caliper Life Sciences, Waltham, MA, USA). For quantification, the bioluminescence light intensity was measured at the region of interest and expressed in relative light units (RLU/min) using Living Image 4.0 (Caliper Life Sciences). To calculate the enhancer activity in the heart, we defined the ratio of heart to brain luciferase intensities as the cardiac-specific enhancer activity.

Transverse aortic constriction (TAC)

Transgenic mice aged 8 wk and weighing 20–25 g were subjected to pressure overload, as described previously (22). Briefly, the chest was entered *via* the second intercostal space at the upper left sternal border. After the arch of the aorta was isolated, a TAC was created using a 7-0 suture tied twice around a 27-gauge needle and the aortic arch, between the innominate and left common carotid arteries. After the suture was tied, the needle was gently removed, yielding 60–80% constriction of the aorta.

PE-induced hypertrophy

Transgenic mice aged 8 wk and weighing 20–25 g were treated with PE (75 mg/kg/d) using an osmotic minipump (Alzet, Cupertino, CA, USA) to induce cardiac hypertrophy, as previously reported (23, 24).

Statistical analysis

Data are expressed as means ± SE. The 2-tailed Student's *t* test and repeated ANOVA were used to analyze differences between the groups. Values of $P < 0.05$ were considered to represent a significant difference.

RESULTS

Identification of candidate enhancers near the *Nppa-Nppb* locus using comparative genomics and ChIP-seq

To identify potential enhancers, we performed a comparative analysis of the genomic sequences of mouse and divergent species and identified CRs that may function as common regulatory sequences (25–27). We defined CRs that were homologous at least in the human and mouse genomes and at least 1 kb away from the transcription start sites of *Nppa* and *Nppb* as the candidate enhancers. First, we analyzed the 50-kb *Nppa-Nppb* locus bounded by the binding sites of 2 CCCTC-binding factors (CTCFs), which can function as insulators (28, 29). Using a genome database (30), we identified 11 CRs, including the *Nppa* and *Nppb* introns in the 50-kb region (**Fig. 1**).

Next, we performed a ChIP-seq analysis on RNA polymerase II and H3K4me3 in the adult mouse heart. We analyzed the epigenetic modifications near the *Nppa* and *Nppb* genes combined with the ChIP-seq analysis using a public database of the adult mouse heart (30). We hypothesized that the normal heart would have activated epigenetic marks because *Nppa* and *Nppb* are expressed, albeit at low levels, in normal conditions. Recent genome-wide studies have determined that enhancers can be defined as DNA sequences bound by the RNA polymerase II and transcriptional coactivator protein p300, and where histone H3 monomethylated at lysine 4 (H3K4me1) accumulates instead of H3K4me3 (31–34). Among the 11 CRs identified, only CR9 coincided with the binding sites of RNA polymerase II and p300, and overlapped with the gene areas modified by H3K4me1, and filled all criteria for the enhancer (Fig. 1). In addition, H3K4me1 modifications in CR9 were only observed in the heart but not in the other organs (Fig. 1 and Supplemental Fig. S1). Therefore, we analyzed the 11 CRs, including CR9, as the most likely distal candidate enhancers for the stress-responsive regulatory regions of the natriuretic peptide genes.

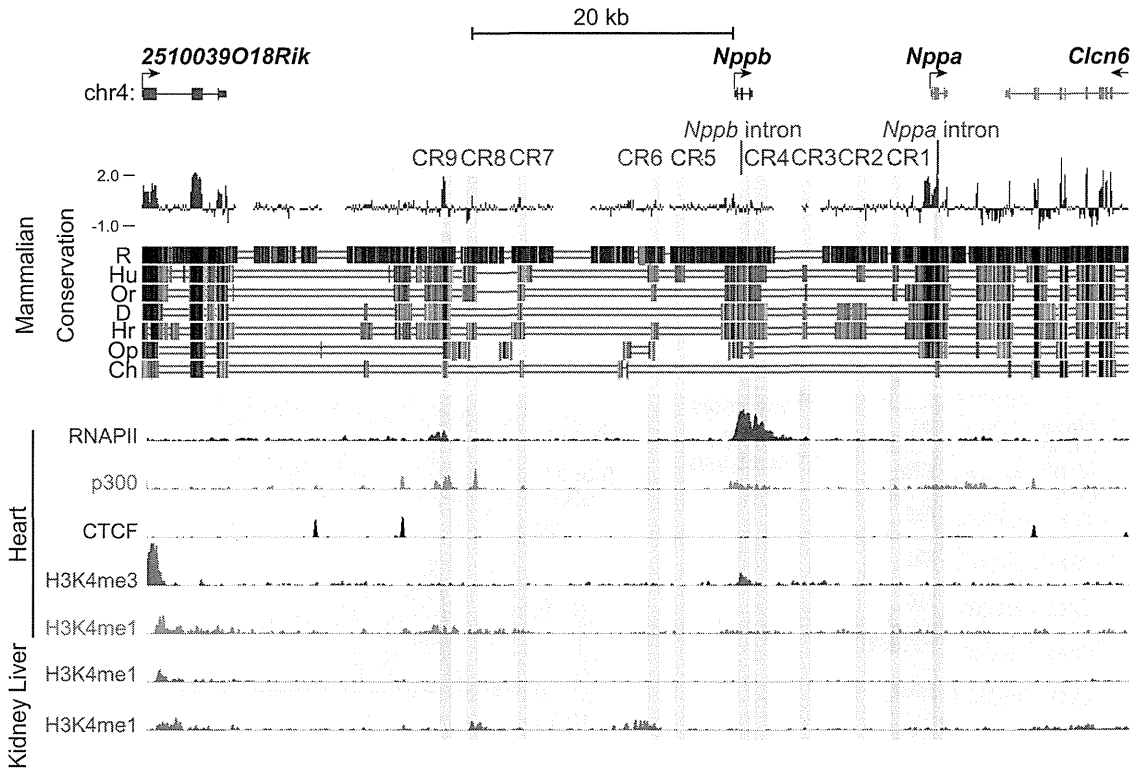

Figure 1. Mammalian evolutionarily conserved regions and ChIP-seq data surrounding the murine *Nppa* and *Nppb* loci. We used an open database on the University of California Santa Cruz (UCSC) Genome Browser to assess the degree of DNA sequence conservation around *Nppa* and *Nppb* gene loci. Blue and red vertical lines, the Placental Mammal Basewise Conservation assessed by PhyloP; black vertical lines, the vertebrate Multiz alignment of DNA sequences among mice and 7 other species (rats, humans, orangutans, dogs, horses, opossums, and chickens). We defined noncoding conserved regions (CRs) that were homologous at least in the human and mouse genomes and at least 1 kb away from the transcription start sites of *Nppa* and *Nppb* as the candidate enhancers. CRs are highlighted as light red vertical bars (CR1-9, *Nppa* intron, and *Nppb* intron). ChIP-seq data for H3K4me1, p300, and CTCF were obtained from an open database of the adult mouse heart. Some CRs coincided with the peaks for H3K4me1, RNA polymerase II, and the transcriptional coactivator protein p300. R, rat; Hu, human; Or, orangutan; D, dog; Hr, horse; Op, opossum; Ch, chicken.

Identification of a distal enhancer element responsive to an α_1-adrenergic receptor agonist

We screened the candidate enhancers for potential stress-responsive regulatory regions. We analyzed the enhancer activity of these 11 CRs after treatment with PE, an α_1-adrenergic receptor agonist, which mimics cardiac overload and induces *Nppa* and *Nppb* expression in cardiomyocytes (35). We confirmed that PE induced the expression of endogenous *Nppa* and *Nppb* specifically in cardiomyocytes but not in cardiac fibroblasts (**Fig. 2*A***). Then, we introduced the 11 CRs with a minimum human cytomegalovirus (CMV) promoter and the luciferase gene into rat cardiomyocytes using a lentiviral vector system.

Among the 11 CRs tested, only CR9, which is located 22 kb upstream from the *Nppb* transcription start site and shows high mammalian conservation score in the Placental Mammal Basewise Conservation by PhyloP (Fig. 2*B*), reproducibly increased the PE-induced luciferase activity by ~5-fold compared to the minimal CMV promoter alone (Fig. 2*C*). However, CR9 did not respond to PE in cardiac fibroblasts (Fig. 2*C*). These results suggest that CR9 is the regulatory element that is responsive to PE specifically in cardiomyocytes.

Long-range physical interaction between the distal enhancer element and the proximal promoters of the *Nppa* and *Nppb* genes

Confirming the looping interactions between distal elements and promoters is one way to demonstrate the transcriptional regulatory activity of distal elements. We performed a 3C assay (20) to comprehensively investigate whether the genomic region containing CR9 moved closer to the *Nppa* or *Nppb* promoter in an adult murine heart treated with a continuous infusion of PE *in vivo*.

The ligation frequencies were quantified by TaqMan real-time PCR using specific primers and probes and were compared to the ligation frequency of noncross-linked *Bam*HI-digested BAC DNA containing the *Nppa-Nppb* locus. We observed that CR9 interacts with both the *Nppa* and *Nppb* promoter regions at a higher frequency relative to other gene areas (Fig. 2*D*); furthermore, PE treatment strengthened these interac-

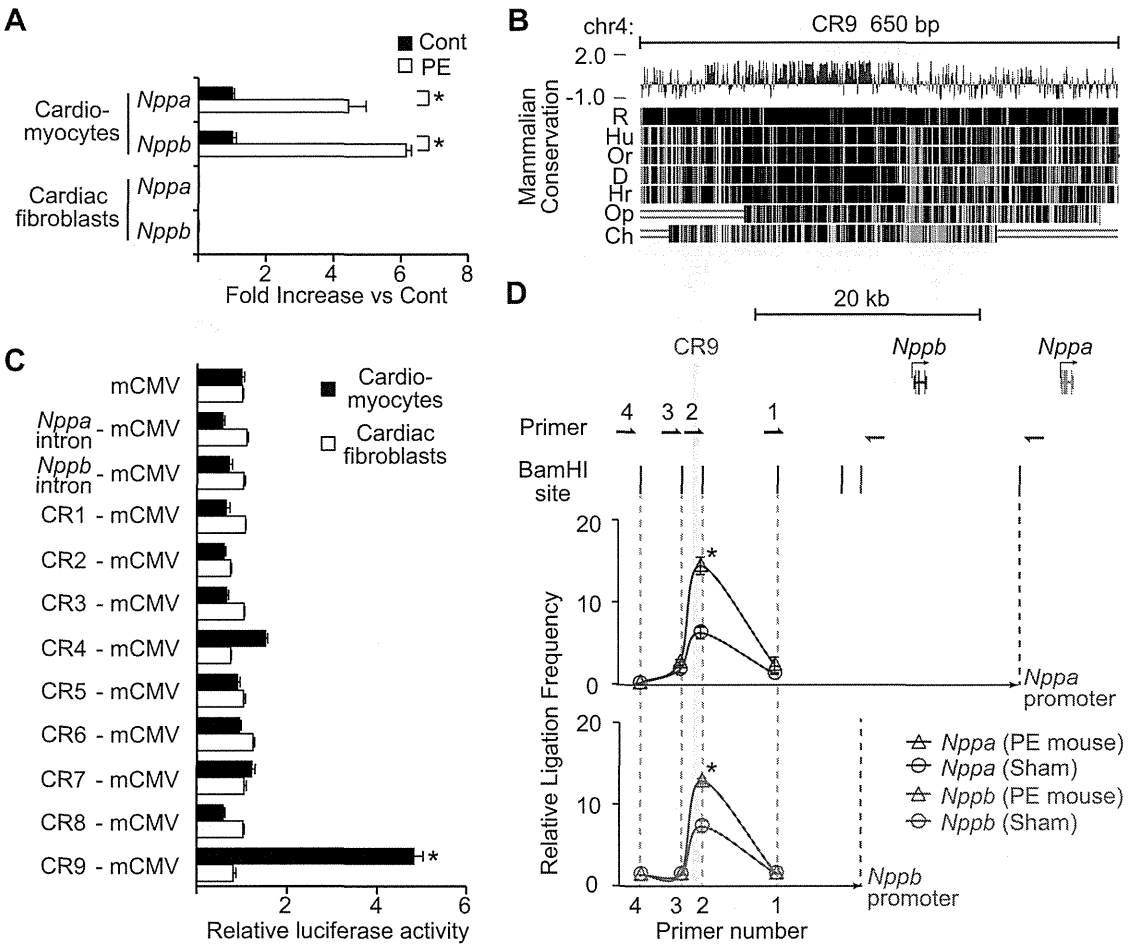

Figure 2. Identification of a distal enhancer element that is responsive to an α_1-adrenergic receptor agonist. *A*) Relative transcript levels of *Nppa* and *Nppb* in rat neonatal cardiomyocytes and cardiac fibroblasts 48 h after treatment with PE (100 μM). Values are means ± SE (n=3 cultures). *$P < 0.01$ *vs.* control; *t* test. *B*) CR9 is a highly conserved genomic region in vertebrates. *C*) Relative luciferase reporter activities of CRs in rat neonatal cardiomyocytes and cardiac fibroblasts 48 h after treatment with PE (100 μM). PE-induced luciferase activity driven by the mCMV promoter was defined as 1. Values are means ± SE (n=5 cultures). *$P < 0.001$ *vs.* mCMV alone; *t* test. *D*) *In vivo* 3C analysis of the murine *Nppa* and *Nppb* loci, showing relative ligation frequencies of each primer to the *Nppa* promoter (blue triangle, mouse with PE treatment; blue circle, mouse without PE) and the *Nppb* promoter (red triangle, mouse with PE treatment; red circle, mouse without PE). Vertical bars and arrows show the positions of *Bam*HI sites and primers. Data were normalized to the amplification value of a *Bam*HI-digested and religated BAC clone, which included the *Nppa* and *Nppb* loci (means ± SE; n=2 hearts). R, rat; Hu, human; Or, orangutan; D, dog; Hr, horse; Op, opossum; Ch, chicken. *$P < 0.05$ *vs.* control; *t* test.

tions (Fig. 2*D*). These results suggest that there is a close proximity between the distal genomic region containing CR9 and the proximal promoters of the *Nppa* and *Nppb* genes in the PE-induced hypertrophic heart.

Establishment of an *in vivo* live imaging system for gene expression in a murine model of heart disease

We confirmed the activity of the newly identified enhancer CR9 in the heart *in vivo*. The conventional histological evaluation of LacZ reporter expression in the heart only provides data at a single time point; therefore, this method cannot be employed for kinetic assessments or time course analyses of reporter expression in a live heart.

To overcome this difficulty, we established a noninvasive and quantitative live imaging system that allowed real-time monitoring of the firefly luciferase reporter. We generated 3 transgenic mouse lines (Tg-line1, Tg-line2, and Tg-line3) in which the CR9 enhancer element and a minimal CMV promoter driving the luciferase reporter gene were introduced into the germline. The live-imaging system detected luciferase expression in the heart, brain, and intestine of the Tg-line1 (**Fig. 3*A***), in the heart, salivary glands, and skin of the Tg-line2 (Supplemental Fig. S2*A*), and in the heart of the Tg-line3 (Supplemental Fig. S2*E*).

To identify the organs in which CR9 functioned as a stress-responsive enhancer, we examined the luciferase reporter expression in each organ by quantitative PCR. Continuous infusion of PE increased the blood pressure and resulted in cardiac hypertrophy (24, 36). The

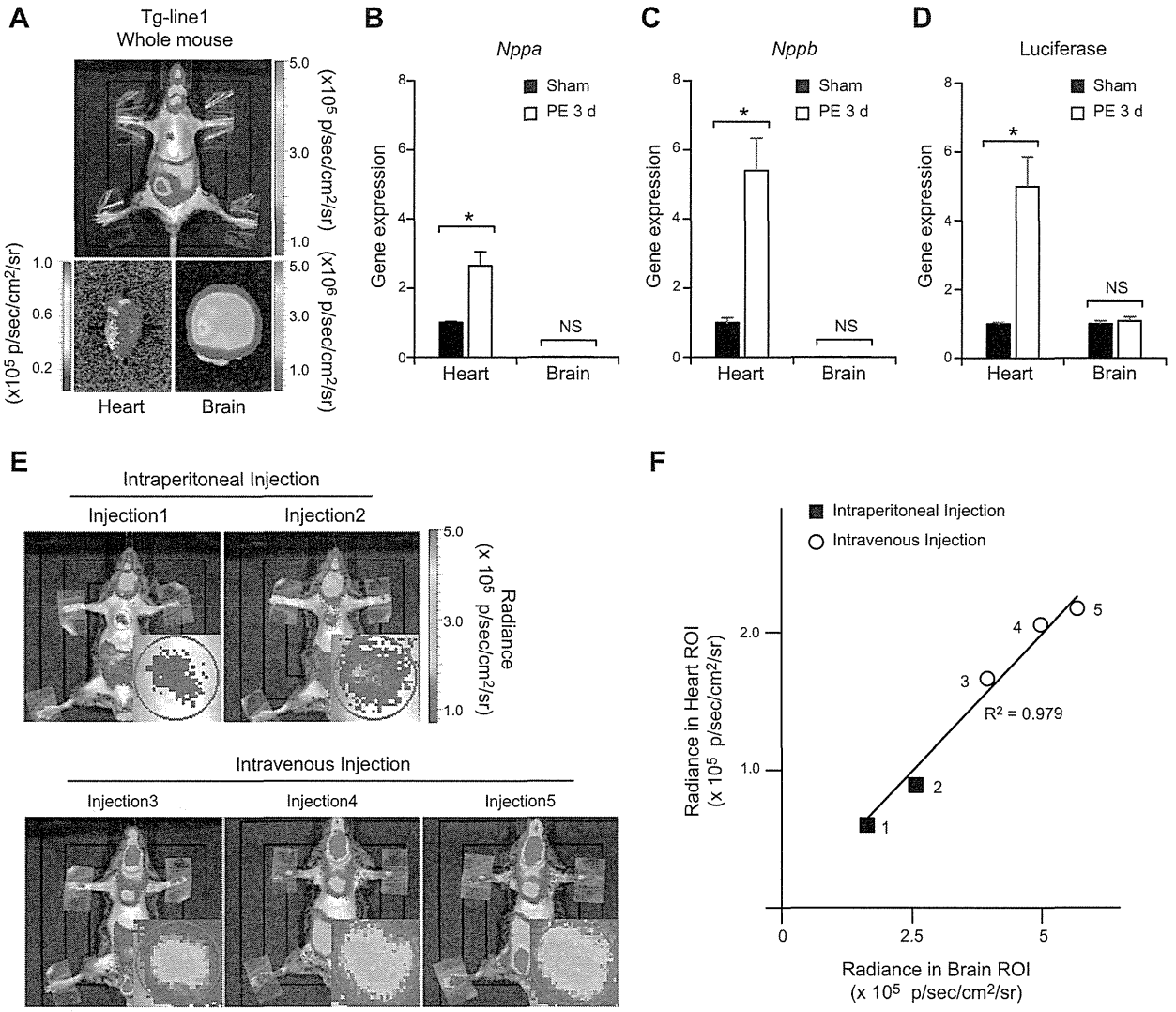

Figure 3. Establishment of an *in vivo* live imaging system for enhancer activity. *A*) Chemiluminescence imaging of CR9 in a mouse of Tg-line1. Top panel: result from whole-animal *in vivo* live imaging. Bottom panels: chemiluminescence images of the heart and brain in the same mouse. *B, C*) Relative transcript levels of *Nppa* and *Nppb* in the ventricular myocardium and brain of CR9 Tg-line1 mice treated with continuous infusion of PE for 3 d. Average transcript level in the ventricular myocardium of preinfused mice was defined as 1 (means ± SE; n=5 hearts). *$P < 0.01$ *vs.* sham-infused mice; *t* test. *D*) Relative transcript levels of luciferase reporter in the ventricular myocardium and brain of the CR9 Tg-line1 mice continuously infused with PE for 3 d. Average transcript level in the ventricular myocardium and brain of preinfused mice was defined as 1. (means ± SE; n=5 hearts). *$P < 0.01$ *vs.* sham-infused mice; *t* test. *E*) Comparison of the chemiluminescence intensities obtained using different luciferin injection methods in a Tg-line1 mouse; injections 1 and 2, intraperitoneal injections (top panels), injections 3, 4, and 5, intravenous injections (bottom panels). Injections were performed ≥4 h apart to eliminate the effect of the previous injection. Inset in each panel shows a magnified image of the heart. *F*) Scatterplots of the chemiluminescence intensities in the heart and brain. Plots indicate the independent experiments shown in each panel in *E*. There is a linear relationship between the expression in the heart and the brain, $R^2 = 0.979$.

expression of endogenous *Nppa* and *Nppb* mRNA increased 3 d after the PE infusion began (Fig. 3*B, C* and Supplemental Fig. S2*B, C, F, G*). Concomitantly, the quantitative PCR analysis of the CR9 luciferase mRNA expression showed enhanced expression in the ventricular myocardium 3 d after the PE infusion (Fig. 3*D* and Supplemental Fig. S2*D, H*). On the other hand, in the brain and the salivary glands where neither *Nppa* nor *Nppb* is highly expressed, the CR9-driven luciferase mRNA expression did not respond to PE (Fig. 3*B–D* and Supplemental Fig. S2*B–D, F–H*). Therefore, the patterns of PE-induced luciferase expression suggest that CR9 is almost exclusively active in the heart. Because the integration sites were random in these three lines, the patterns of luciferase expression depend on CR9 or other enhancers near the integrated sites. The expression of luciferase in the brain of Tg-line1 and salivary glands of Tg-line2, both of which express neither *Nppa* nor *Nppb,* might be driven by other enhancers near the integrated sites.

To evaluate the accuracy and reproducibility of this method, we measured the luminescence in the heart of

a mouse from Tg-line1. In this transgenic line, the brain, intestine, and testis expressed the reporter protein due to positional effects of the insertion site and most likely not due to CR9 activity. Because the luciferase mRNA expression in the brain remained unchanged after PE treatment (Fig. 3*D*), we used the reporter activity in the brain as a control. The absolute luminescence values of the heart were affected by the injection method and the amount of luciferase substrate injected (Fig. 3*E*). However, using brain luminescence as a control, we successfully eliminated the signal variations caused by these differences. The ratio of the luminescence in the heart and brain remained constant within each mouse, independent of the injection method (Fig. 3*F*). Therefore, we defined the ratio of heart to brain luciferase intensities as the cardiac-specific enhancer activity.

Distal enhancer element was activated in the murine model of heart failure

To examine whether the CR9 enhancer was also responsible for gene expression in other pathological conditions, we subjected Tg-line1 mice to heart failure induced by TAC and compared them with sham-surgery mice. This model mimics the heart condition of patients with hypertension who suffer a continuous pressure overload on the heart. The pressure overload by TAC caused potent cardiac hypertrophy at 2 wk postsurgery and reduced cardiac contractility at 3 wk postsurgery (**Fig. 4*A, B***), as previously reported (22). The endogenous *Nppa* and *Nppb* expression increased severalfold in the ventricular myocardium 3 wk after the TAC surgery (Fig. 4*C*). The heart to brain luciferase intensity ratio also increased severalfold 3 wk following the TAC surgery (Fig. 4*D, E* and Supplemental Fig. S3). However, the heart to brain luciferase intensity ratio of sham-surgery mice did not change after the surgery (Fig. 4*D, E* and Supplemental Fig. S3; 3 wk after TAC surgery: 5.7±1.3 fold; 3 wk after sham surgery: 1.0±0.2 fold; $P < 0.001$, repeated ANOVA). These results suggest that CR9 increases transcriptional activity during mechanical pressure overload-induced hypertrophy and subsequent heart failure.

DISCUSSION

Here, we focused on the stress-responsive regulatory elements of *Nppa* and *Nppb* in heart failure. By screening the evolutionarily conserved and epigenetically modified regions around the *Nppa* and *Nppb* gene loci, we identified a 650-bp transcriptional enhancer that was responsive to an α_1-adrenergic receptor agonist *in vitro*. Furthermore, *in vivo* 3C analysis revealed that this distal enhancer directly interacted with the 5′-flanking regions of both *Nppa* and *Nppb*. Using *in vivo* live imaging of luciferase reporter gene expression, we observed that this 650-bp enhancer caused cardiac-specific activation of reporter gene expression during the progression of pressure overload-induced heart failure. Notably, this is the first study to provide a time series analysis for monitoring enhancer activity under pathological conditions in an individual live mouse.

Although numerous approaches have been used to explore the stress-responsive regulatory elements driving gene transcription during heart failure (11, 12, 14), these elements have not yet been identified due to the technical difficulty involved. To detect the elements that are responsive to pathological conditions such as heart failure, it is essential to confirm the activity of the responsive element using a beating heart that remains connected to the systemic cardiovascular system. Therefore, it would be beneficial to establish transgenic mouse lines carrying a reporter plasmid to assess the responsive elements driving the expression of specific genes. However, the creation of multiple stable adult mouse lines to identify these elements is time-consuming.

In this study, we utilized two improved methods for reporter analysis and successfully identified a novel potent enhancer.

First, by performing an enhancer analysis using a lentiviral vector, we accurately identified candidate enhancers in cardiomyocytes and subsequently generated transgenic reporter mice. Previous promoter analyses used electroporation or lipofection to transfect cultured cardiomyocytes with plasmids (37, 38), but the transfection efficiency of these methods in primary cardiomyocytes is too low to accurately measure reporter activity during the stress response. In this study, greater than 90% transduction efficiency of cardiomyocytes was achieved using a lentiviral vector, which enabled us to accurately identify a specific enhancer fragment. Using this method, we efficiently minimized the number of reporter plasmids to be subsequently integrated into the mouse genome to screen for potential enhancers.

Second, by sequentially measuring the enhancer activity in a single live mouse, we collected robust data to assess enhancer activity in the heart *in vivo*. LacZ is not a suitable reporter for this purpose because LacZ activity can only be assessed after animal euthanization. Therefore, we overcame this limitation using the luciferase reporter plasmid. Recent advances in high-sensitivity luminescence imaging have made it possible to evaluate enhancer-driven luciferase activity without operating on the mice. Therefore, we sequentially assessed reporter activity and hemodynamic changes in the same mouse throughout the time course of the development of heart failure. These data were highly reproducible and enabled us to identify an enhancer element that was activated by cardiac overload. Because this method can be applied to any organ, the *in vivo* luciferase reporter assay may be used for assessing the *in vivo* enhancer or promoter activities responsible for clinically important diseases. The noninvasive nature of this method also enabled us to simultaneously assess the hemodynamic and metabolic parameters *in vivo* along with reporter activity. Specifically, the Tg-line1

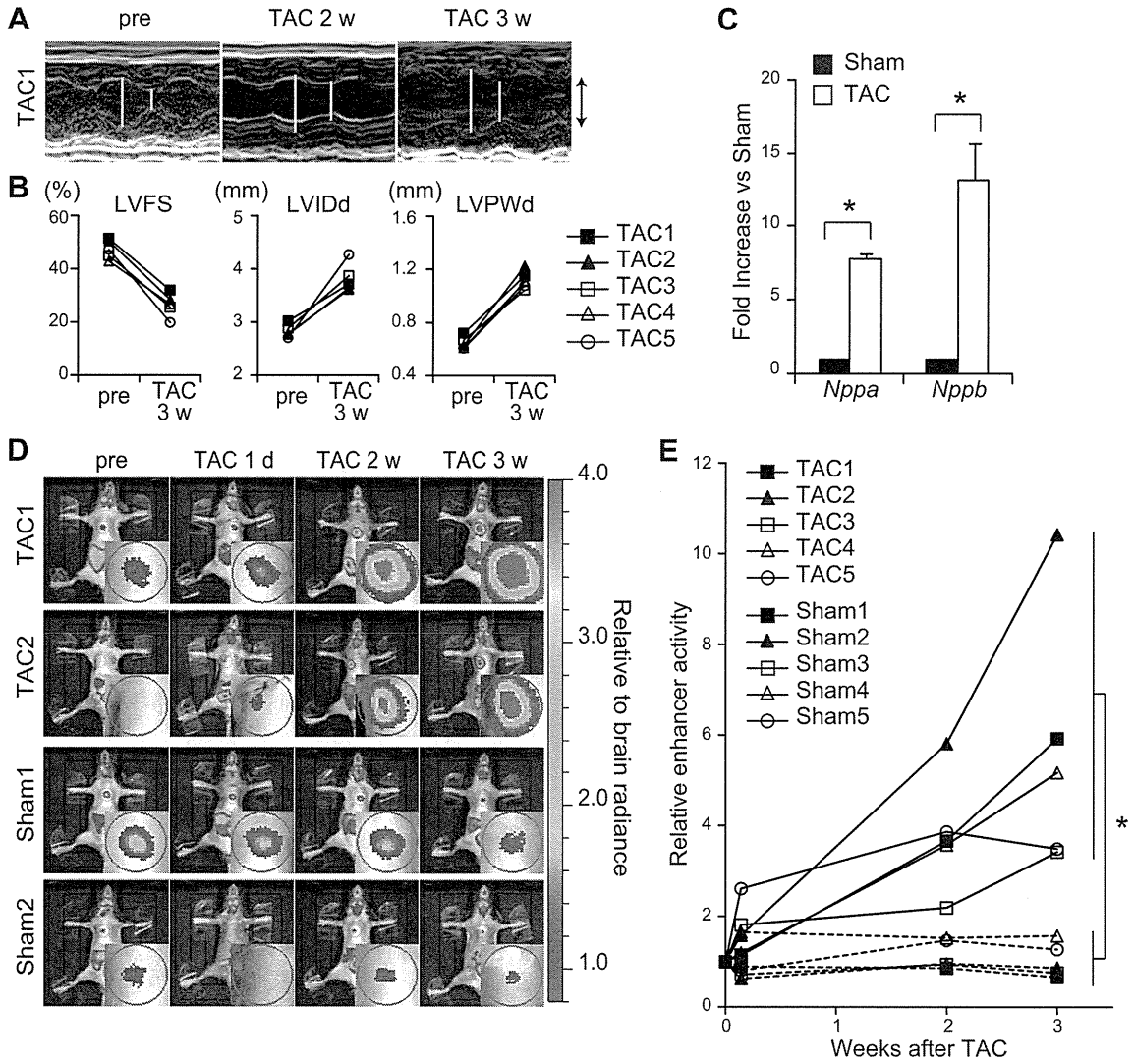

Figure 4. Distal enhancer element is reactivated in the murine model of heart failure. *A*) Representative M-mode echocardiograms in a mouse of Tg-line1 (TAC1) before and after TAC. Open bars indicate maximal left ventricular internal dimension in diastole (LVIDd) and maximal left ventricular internal dimension in systole (LVIDs). Up and down arrows represent 3 mm. *B)* Echocardiographic changes in left ventricular fractional shortening (LVFS), LVIDd, and left ventricular posterior wall thickness in diastole (LVPWd) in 5 mice of Tg-line1 (TAC1-5) before and after TAC. *C*) Relative *Nppa* and *Nppb* transcript levels in the ventricular myocardium 3 wk after the TAC procedure (means ± SE; n=3 hearts). *$P < 0.05$ *vs.* sham-surgery mice; *t* test. *D*) Sequential *in vivo* live imaging of 4 representative Tg-line1 mice before and after TAC or sham surgery at each time point. Top 2 and bottom 2 panels represent sequential imaging data of TAC and sham-surgery mice, respectively. Sequential imaging of the 6 other surgically treated mice is shown in Supplemental Fig. S3. Insets in images show magnified images of the heart. Color scale depends on the ratio relative to brain intensity. *E*) Cardiac-specific enhancer activity plots of 10 Tg-line1 mice (TAC1, TAC2, and Sham1, Sham2, shown in *D*) and TAC3–5 and Sham3–5 shown in Supplemental Fig. S3). Heart to brain luciferase intensity ratio represents the cardiac-specific enhancer activity; enhancer activity in presurgery mice was defined as 1. 3 wk after TAC surgery: 5.7 ± 1.3 fold; 3 wk after sham surgery: 1.0 ± 0.2 fold; means ± SE; n = 5. *$P < 0.001$, repeated ANOVA.

mice enabled us to accurately quantify the expression level of the natriuretic peptides. These mice are useful tools for repeatedly assessing the degree of heart failure to screen various cardiovascular drugs.

The integration of activities from multiple enhancers could confer specificity and robustness to transcriptional regulation (1). Warren *et al.* (14) identified the *Nppa* enhancer in the embryonic heart by examining Nkx2-5 binding regions around the *Nppa* locus, but the enhancer did not respond to heart failure. This enhancer does not overlap with CR9 and might regulate *Nppa* expression only during the embryonic stage (14). On the other hand, Horsthuis *et al.* (11) showed that the regulatory region from −27 to +58 kb relative to the transcription start site of *Nppa* was sufficient for *Nppa* gene expression in the failing heart, similar to CR9. However, because this 85-kb regulatory region does not include CR9, *Nppa* may have multiple enhanc-

ers that regulate its expression during heart failure. Furthermore, the length of the 85-kb region poses a challenge for understanding its specific biological role.

This is the first study to provide a time course imaging analysis of enhancer activity using an individual live diseased mouse model. Using this new method, we identified a novel heart enhancer. This method can be widely used for identifying enhancers that regulate transcriptional activity only under pathological conditions. FJ

This research was supported by the Japan Society for the Promotion of Science (JSPS) through the Funding Program for Next Generation World-Leading Researchers (NEXT Program), which was initiated by the Council for Science and Technology Policy (CSTP); grants-in-aid from the Ministry of Health, Labor, and Welfare of Japan; grants-in-aid from the Ministry of Education, Culture, Sports, Science, and Technology of Japan; and grants-in-aid from the Japan Society for the Promotion of Science. This research was also supported by grants from the Japan Heart Foundation, the Japan Cardiovascular Research Foundation, the Japan Medical Association, the Japan Intractable Diseases Research Foundation, the Uehara Memorial Foundation, the Takeda Science Foundation, the Ichiro Kanehara Foundation, the Inoue Foundation for Science, the Mochida Memorial Foundation, a Heart Foundation/Novartis Grant for Research Award on Molecular and Cellular Cardiology, the Japan Foundation of Applied Enzymology, the Naito Foundation, the Banyu Foundation, and Showa Houkoukai. The authors thank Hiroshi Kimura for antibodies, Seitaro Nomura for the ChIP-seq analysis, Saori Ikezawa and Eri Takata for technical assistance, and Yuko Okada and Hiromi Fujii for secretarial support.

REFERENCES

1. Spitz, F., and Furlong, E. E. (2012) Transcription factors: from enhancer binding to developmental control. *Nat. Rev. Genet.* **13,** 613–626
2. Chien, K. R., Domian, I. J., and Parker, K. K. (2008) Cardiogenesis and the complex biology of regenerative cardiovascular medicine. *Science* **322,** 1494–1497
3. Olson, E. N. (2006) Gene regulatory networks in the evolution and development of the heart. *Science* **313,** 1922–1927
4. Burley, D. S., and Baxter, G. F. (2007) B-type natriuretic peptide at early reperfusion limits infarct size in the rat isolated heart. *Basic Res. Cardiol.* **102,** 529–541
5. Holtwick, R., van Eickels, M., Skryabin, B. V., Baba, H. A., Bubikat, A., Begrow, F., Schneider, M. D., Garbers, D. L., and Kuhn, M. (2003) Pressure-independent cardiac hypertrophy in mice with cardiomyocyte-restricted inactivation of the atrial natriuretic peptide receptor guanylyl cyclase-A. *J. Clin. Invest.* **111,** 1399–1407
6. Kitakaze, M., Asakura, M., Kim, J., Shintani, Y., Asanuma, H., Hamasaki, T., Seguchi, O., Myoishi, M., Minamino, T., Ohara, T., Nagai, Y., Nanto, S., Watanabe, K., Fukuzawa, S., Hirayama, A., Nakamura, N., Kimura, K., Fujii, K., Ishihara, M., Saito, Y., Tomoike, H., and Kitamura, S. (2007) Human atrial natriuretic peptide and nicorandil as adjuncts to reperfusion treatment for acute myocardial infarction (J-WIND): two randomised trials. *Lancet* **370,** 1483–1493
7. Li, P., Wang, D., Lucas, J., Oparil, S., Xing, D., Cao, X., Novak, L., Renfrow, M. B., and Chen, Y. F. (2008) Atrial natriuretic peptide inhibits transforming growth factor beta-induced Smad signaling and myofibroblast transformation in mouse cardiac fibroblasts. *Circ. Res.* **102,** 185–192
8. Tamura, N., Ogawa, Y., Chusho, H., Nakamura, K., Nakao, K., Suda, M., Kasahara, M., Hashimoto, R., Katsuura, G., Mukoyama, M., Itoh, H., Saito, Y., Tanaka, I., Otani, H., and Katsuki, M. (2000) Cardiac fibrosis in mice lacking brain natriuretic peptide. *Proc. Natl. Acad. Sci. U. S. A.* **97,** 4239–4244
9. De Lange, F. J., Moorman, A. F., and Christoffels, V. M. (2003) Atrial cardiomyocyte-specific expression of Cre recombinase driven by an Nppa gene fragment. *Genesis* **37,** 1–4
10. Habets, P. E., Moorman, A. F., Clout, D. E., van Roon, M. A., Lingbeek, M., van Lohuizen, M., Campione, M., and Christoffels, V. M. (2002) Cooperative action of Tbx2 and Nkx2.5 inhibits ANF expression in the atrioventricular canal: implications for cardiac chamber formation. *Genes Dev.* **16,** 1234–1246
11. Horsthuis, T., Houweling, A. C., Habets, P. E., de Lange, F. J., el Azzouzi, H., Clout, D. E., Moorman, A. F., and Christoffels, V. M. (2008) Distinct regulation of developmental and heart disease-induced atrial natriuretic factor expression by two separate distal sequences. *Circ. Res.* **102,** 849–859
12. Knowlton, K. U., Rockman, H. A., Itani, M., Vovan, A., Seidman, C. E., and Chien, K. R. (1995) Divergent pathways mediate the induction of ANF transgenes in neonatal and hypertrophic ventricular myocardium. *J. Clin. Invest.* **96,** 1311–1318
13. Small, E. M., and Krieg, P. A. (2003) Transgenic analysis of the atrialnatriuretic factor (ANF) promoter: Nkx2-5 and GATA-4 binding sites are required for atrial specific expression of ANF. *Dev. Biol.* **261,** 116–131
14. Warren, S. A., Terada, R., Briggs, L. E., Cole-Jeffrey, C. T., Chien, W. M., Seki, T., Weinberg, E. O., Yang, T. P., Chin, M. T., Bungert, J., and Kasahara, H. (2011) Differential role of Nkx2-5 in activation of the atrial natriuretic factor gene in the developing versus failing heart. *Mol. Cell. Biol.* **31,** 4633–4645
15. Simpson, P., McGrath, A., and Savion, S. (1982) Myocyte hypertrophy in neonatal rat heart cultures and its regulation by serum and by catecholamines. *Circ. Res.* **51,** 787–801
16. Siepel, A., Bejerano, G., Pedersen, J. S., Hinrichs, A. S., Hou, M., Rosenbloom, K., Clawson, H., Spieth, J., Hillier, L. W., Richards, S., Weinstock, G. M., Wilson, R. K., Gibbs, R. A., Kent, W. J., Miller, W., and Haussler, D. (2005) Evolutionarily conserved elements in vertebrate, insect, worm, and yeast genomes. *Genome Res.* **15,** 1034–1050
17. Blanchette, M., Kent, W. J., Riemer, C., Elnitski, L., Smit, A. F., Roskin, K. M., Baertsch, R., Rosenbloom, K., Clawson, H., Green, E. D., Haussler, D., and Miller, W. (2004) Aligning multiple genomic sequences with the threaded blockset aligner. *Genome Res.* **14,** 708–715
18. Pollard, K. S., Hubisz, M. J., Rosenbloom, K. R., and Siepel, A. (2010) Detection of nonneutral substitution rates on mammalian phylogenies. *Genome Res.* **20,** 110–121
19. Zhang, Y., Liu, T., Meyer, C. A., Eeckhoute, J., Johnson, D. S., Bernstein, B. E., Nusbaum, C., Myers, R. M., Brown, M., Li, W., and Liu, X. S. (2008) Model-based analysis of ChIP-Seq (MACS). *Genome Biol.* **9,** R137
20. Dekker, J., Rippe, K., Dekker, M., and Kleckner, N. (2002) Capturing chromosome conformation. *Science* **295,** 1306–1311
21. Hagege, H., Klous, P., Braem, C., Splinter, E., Dekker, J., Cathala, G., de Laat, W., and Forne, T. (2007) Quantitative analysis of chromosome conformation capture assays (3C-qPCR). *Nat. Protoc.* **2,** 1722–1733
22. Liao, Y., Ishikura, F., Beppu, S., Asakura, M., Takashima, S., Asanuma, H., Sanada, S., Kim, J., Ogita, H., Kuzuya, T., Node, K., Kitakaze, M., and Hori, M. (2002) Echocardiographic assessment of LV hypertrophy and function in aortic-banded mice: necropsy validation. *Am. J. Physiol. Heart Circ. Physiol.* **282,** H1703–H1708
23. Saadane, N., Alpert, L., and Chalifour, L. E. (1999) Expression of immediate early genes, GATA-4, and Nkx-2.5 in adrenergic-induced cardiac hypertrophy and during regression in adult mice. *Brit. J. Pharmacol.* **127,** 1165–1176
24. Vecchione, C., Fratta, L., Rizzoni, D., Notte, A., Poulet, R., Porteri, E., Frati, G., Guelfi, D., Trimarco, V., Mulvany, M. J., Agabiti-Rosei, E., Trimarco, B., Cotecchia, S., and Lembo, G. (2002) Cardiovascular influences of α1β-adrenergic receptor defect in mice. *Circulation* **105,** 1700–1707
25. Nobrega, M. A., Ovcharenko, I., Afzal, V., and Rubin, E. M. (2003) Scanning human gene deserts for long-range enhancers. *Science* **302,** 413
26. Thomas, J. W., Touchman, J. W., Blakesley, R. W., Bouffard, G. G., Beckstrom-Sternberg, S. M., Margulies, E. H., Blanchette, M., Siepel, A. C., Thomas, P. J., McDowell, J. C., Maskeri, B., Hansen, N. F., Schwartz, M. S., Weber, R. J., Kent, W. J.,